

A SOURCE OF COHERENT SOFT X-RAY RADIATION BASED ON HIGH-ORDER HARMONIC GENERATION AND FREE ELECTRON LASERS*

M. Gullans, J. Wurtele, UC Berkeley, Berkeley, CA, USA,
G. Penn, A. Zholents, LBNL, Berkeley, CA, USA

Abstract

We examine a scheme for a Free Electron Laser (FEL) harmonic amplifier seeded by a 30-nm wavelength signal produced using a process of High-order Harmonic Generation (HHG). The seed is first amplified in an optical klystron from 100 kW to 30 MW using a 1 GeV electron beam and then is used for an energy modulation of electrons in the downstream undulator. Subsequently, a 100-MW level of radiation at shorter wavelengths down to 4 nm is obtained by bunching the energy modulated electrons and passing the bunched beam through an undulator tuned to the desired harmonic of 30 nm.

INTRODUCTION

The process of high-order harmonic generation (HHG) is now routinely used for the generation of laser-like pulses in the extreme ultraviolet (EUV) (see [1] and references therein). The repetition rate of these pulses depends on that of the Ti:Sapphire laser which drives the HHG process, and pulses containing up to 2.5 nJ of energy have been demonstrated with a repetition rate of the order of 1 kHz. Higher pulse energies have also been demonstrated, but at much lower repetition rate. These EUV pulses provide an attractive alternative to optical and vacuum ultraviolet (VUV) pulses for use as a seed signal in FELs employing a harmonic cascade technique [2, 3].

In order to evaluate the potential of HHG to produce an EUV seed for FELs, we consider a specific example of an EUV pulse having a central wavelength of 30 nm, a pulse duration of 25 fs (FWHM of intensity), and a peak power of 100 kW. We also assume that the pulse is transversely and temporally coherent. The FEL uses this seed to produce soft x-rays in the "water window" around 4 nm.

We assume an electron beam energy of 1 GeV. The nominal beam parameters are 500 A current, 1.2 micron normalized emittance, and 75 keV uncorrelated energy spread. The typical electron beam radius is 60 μm . This electron beam enters an optical klystron [4] consisting of an undulator modulator, magnetic chicane and undulator radiator. The undulator period is 3 cm, and each undulator is 1.8 m long. The laser seed is focused to a waist of 120 micron radius in the midpoint of the undulator modulator. This optical klystron amplifies the HHG signal, resulting in a much stronger energy modulation on the electron beam compared

to the case where the same total length of undulator is used as a simple modulator without a magnetic chicane. The modulated beam is then bunched in another magnetic chicane, and radiates at a higher harmonic of the HHG signal in the final undulator. This undulator has a period of 1.5 cm, is 12 m long, and is tuned to the eighth harmonic of the HHG seed, or 3.75 nm wavelength. The break sections between undulators are each 1 m long. The first break section contains a dispersive element generating an R_{56} of 30 microns. The second break section has another dispersive element with an R_{56} of 7.5 microns, to yield bunching at the eight harmonic. A sketch of the configuration is shown in Figure 1. Except for the use of the optical klystron, this design is similar to earlier designs for producing FEL output at a harmonic of a laser seed [5, 6].

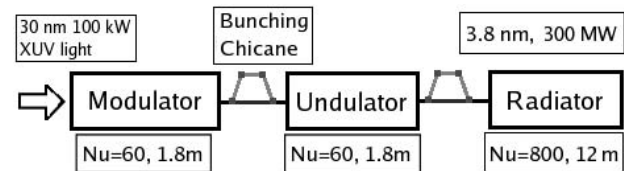


Figure 1: Sketch of a configuration for an FEL seeded with an HHG pulse. Each pair of undulators are separated by 1 m, which contains a dispersive section. The first two undulators have a period of 3 cm, the final undulator has a period of 1.5 cm and is resonant with the eighth harmonic of the HHG pulse.

FEL PERFORMANCE

Simulations were performed using GENESIS [7], which allows for either single-slice simulations or time-dependent runs. The undulators are tuned by adjusting the normalized undulator parameter, a_U , defined as $a_U \equiv eB_{RMS}\lambda_U/2\pi m_e c$, where λ_U is the undulator period. The FEL must approximately satisfy the resonance condition given by $\lambda \approx \lambda_U(1 + a_U^2)/2\gamma^2$, where λ is the radiation wavelength and γ is the energy in units of the electron rest mass energy [8].

The lattice designs were optimized by first running single-slice simulations, and the same configurations were then used for full time-dependent runs. While the beam parameters used are somewhat challenging, they are required to achieve seeded FEL performance which rises above shot noise levels. The energy spread, σ_γ , is a critical parameter for generation of harmonics, as reflected by the

*This work was supported by the Director, Office of Science, High Energy Physics, U. S. Department of Energy under Contract No. DE-AC02-05CH11231.

requirement that $\sigma_\gamma/\gamma < \rho$ for proper FEL performance [9], where ρ is the Pierce parameter related to the tolerance of the FEL to deviations from the resonance condition. We have chosen a small value for σ_γ rather than increasing the electron energy, which would add significant costs to an FEL.

Results from single-slice simulations are shown in Figure 2, which displays the logarithmic power along the final radiator for the main configuration and for reduced values of the transverse emittance (ϵ_N). These results are summarized in Table 1. Transverse emittances of 1.2 μm , 1.0 μm , and 0.8 μm are used, while the beam radius (r) is adjusted to preserve a constant beta of around 6 m. These cases were optimized by varying a_U in each undulator and the strength of the bunching chicane magnets. For the nominal case, the initial bunching in the final undulator is 4.3 %, the initial energy spread is 320 keV, the power at 2 m is 2.0 MW, the peak power is 290 MW and the gain length L_G is 1.7 m, where $1/L_G$ is the typical value of $(1/P)dP/dz$ during the period of exponential growth in output power. This gain length corresponds to a Pierce parameter of roughly 7×10^{-4} .

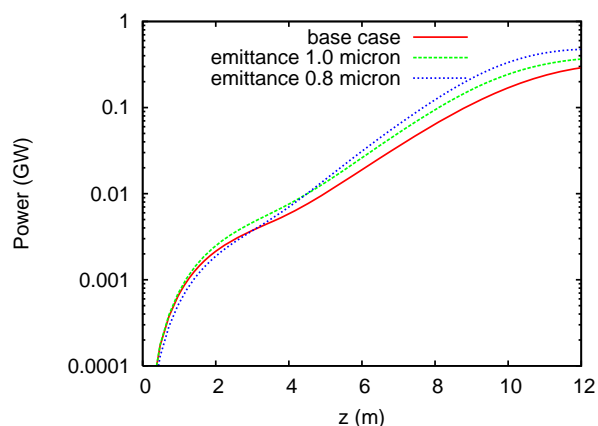


Figure 2: Power along final radiator for different transverse emittances.

Table 1: Effects of changing beam parameters on FEL performance, after tuning. The nominal parameters used: $\epsilon_N = 1.2 \mu\text{m}$, $\gamma = 1.0 \text{ GeV}$, $I = 500 \text{ A}$, and $\sigma_\gamma = 75 \text{ keV}$.

ϵ_N (μm)	Initial Bunch (%)	Power: 2 m (MW)	Power: End (MW)	L_G (m)
1.2	4.3	2.0	290	1.7
1.0	4.1	2.3	366	1.6
0.8	3.3	1.8	474	1.4

Qualitatively, we can see from Fig. 2 that the FEL is operating in the high-gain regime for all the different parameter choices. In each simulation, the power starts off with quadratic growth determined by the initial bunching, then between 3 and 4 m the power begins to grow exponentially, with gain length L_G . This is correlated with exponential

growth in the bunching factor, until the bunching reaches a peak and the beam begins to de-bunch leading to the saturation regime for power growth. The power has saturated by the end of the radiator.

Another consideration is the dependence of the performance on the input laser power. Fig. 3 exhibits the output power resulting from changes in input power from the nominal value of 100 kW. As usual for a harmonic generation scheme, the output power drops essentially to zero at some cutoff power (around 20 kW). The output power is fairly insensitive to the input laser power down to 75 kW, and a 10 % variation in laser power leads to a 5 % decrease in the peak output power. These results give a rough idea of the temporal shape of the output pulse given the input laser seed, which are studied more accurately below using full time-dependent simulations.

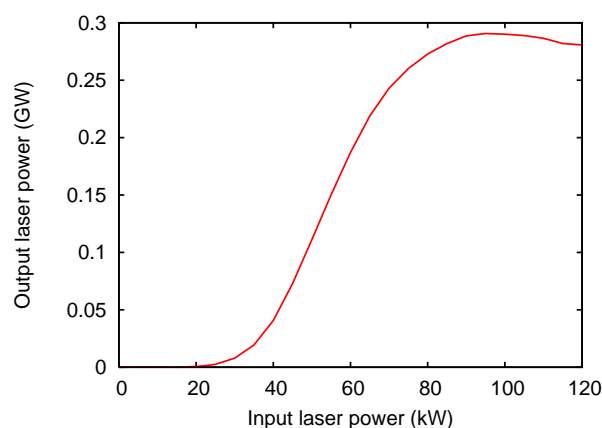


Figure 3: The output power as a function of the input power, tuned for a 100 kW input.

Time-dependent FEL simulations were performed for a constant beam profile and a Gaussian HHG laser seed with a 25 fs FWHM and peak power of 100 kW. The peak laser power overlaps the electron beam at the point marked as $t = 0$ on the scale in Fig. 4. The displacement of the final output is due to slippage of the electron beam with respect to the laser fields. The studies were carried out for a ratio of σ_γ/γ of 7.5×10^{-5} , using an ϵ_N of 1.2 μm , 1.0 μm , and 0.8 μm . The FEL configuration is identical to that used from the single-slice simulations. Table 2 and Fig. 4 summarize the simulation results.

Table 2: Summary of the time-dependent simulation results.

ϵ_N (μm)	Peak Power (MW)	FWHM in spectrum
1.2	310	0.046%
1.0	460	0.045%
0.8	660	0.043%

There are several qualitative similarities in the power plots as shown Fig. 4. Foremost is the asymmetry in the

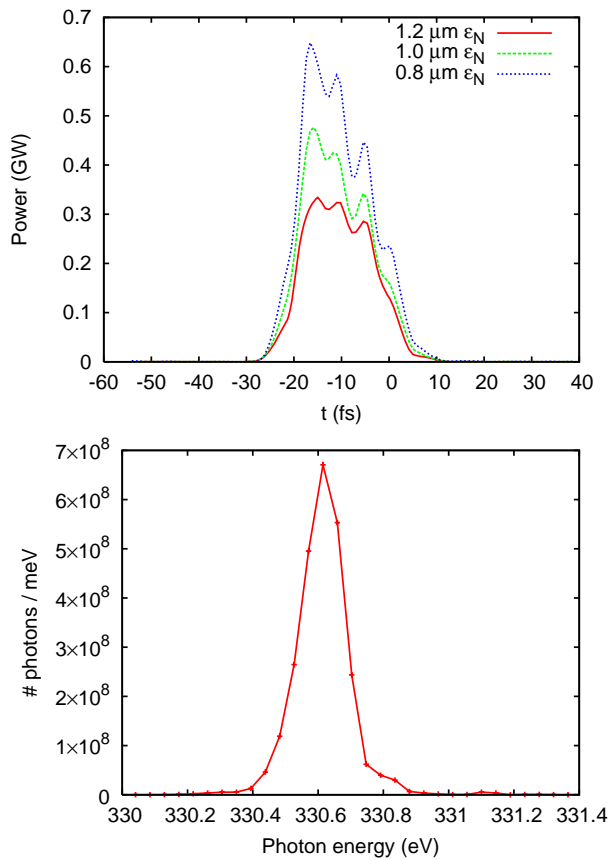


Figure 4: The top graph shows the power profile at the end of the FEL as a function of longitudinal position for various examples, while the bottom graph shows the spectrum for the 1.2 μm ϵ_N case. The spectra in the other examples are similar except for their magnitude, as is expected since the spread in frequency is largely determined by short duration of the pulse.

FEL output, with peak power at the leading edge of the pulse that is even more than predicted from single-slice simulations. The average power within the core of the pulse is in reasonable agreement with the single-slice simulation results. The ubiquitous appearance of this feature suggests that this is an intrinsic characteristic of this FEL scheme when seeded with such a short Gaussian laser pulse. Another interesting feature is the dramatic rise in peak power between the 1.2 and 0.8 μm emittance cases, almost by a factor of two.

We can estimate the longitudinal coherence of the output laser pulse by comparing the observed FWHM in the spectrum with the expected FWHM assuming a perfect Gaussian output power profile with the same FWHM as measured in Fig. 4. The result of this calculation is that the FWHM in the observed spectrum is about 1.8 times larger than the calculated FWHM based on the above assumptions. Separately and in addition to phase variations, sharp variations in power also suggest a lack of longitudinal coherence. Consequently, this is a reasonable result for longi-

tudinal coherence, since our output power profile has several peaks in each case.

CONCLUSIONS

We have presented the results of several FEL simulations using a low-power HHG laser as a seed for a harmonic generation FEL with high gain. It was found that suitable choices of parameters, which are somewhat aggressive but reasonable, yield robust simulation results and good laser output. Full time-dependent simulations have been performed for several examples based on these two approaches.

REFERENCES

- [1] H.C. Kapteyn, M.M. Murnane, and I.P. Christov, *Physics Today* (March 2005) 39–44.
- [2] G. Lambert, B. Carré, M.E. Couprie, D. Garzella, et al., *Proceedings of the 26th International Free Electron Laser Conference (FEL04)*, Trieste, Italy (2004), paper MOPOS21.
- [3] B.W.J. McNeil, G.R.M. Robb, N.R. Thompson, J. Jones, et al., *Proceedings of the 27th International Free Electron Laser Conference (FEL05)*, Stanford, CA, USA (2005), paper THPP025.
- [4] R. Bonifacio, R. Corsini, and P. Pierini, *Physical Review A* **45** (1992), 4091–4096.
- [5] L.-H. Yu, M. Babzien, I. Ben-Zvi, L. F. DiMauro, et al., *Science* **289** (2000), 932–934.
- [6] L.-H. Yu, L. F. DiMauro, A. Doyuran, W. S. Graves, et al., *Physical Review Letters* **91** (2003), 074801.
- [7] S. Reiche, *Nucl. Instr. Methods A* **429** (1999), 243–248.
- [8] G. Dattoli, A. Renieri, and A. Torre, *Lectures on the Free Electron Laser Theory and Related Topics* (World Scientific, Singapore, 1993).
- [9] R. Bonifacio, C. Pellegrini, and L. M. Narducci, *Optics Communications* **50** (1984), 373–378.